

Simple Approach for Selective Crystal Growth of Intermetallic Clathrates

Stevce Stefanoski,[†] Matt Beekman,[†] Winnie Wong-Ng,[‡] Peter Zavalij,[§] and George S. Nolas^{*,†}

[†]Department of Physics, University of South Florida, 4202 East Fowler Avenue, Tampa, Florida 33620, United States

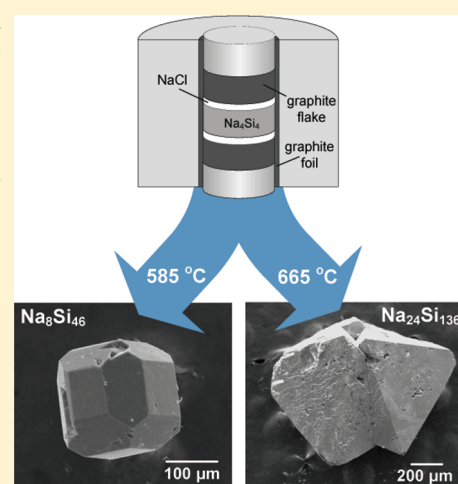
[‡]Materials Science and Engineering Laboratory, National Institute of Standards and Technology, 100 Bureau Drive, Stop 8500, Gaithersburg, Maryland 20899, United States

[§]Department of Chemistry and Biochemistry, University of Maryland, 091 Chemistry Building, College Park, Maryland 20742, United States

 Supporting Information

ABSTRACT: We report on a new method for the synthesis of single-crystal intermetallic clathrates. Alkali-metal is slowly removed from an alkali-silicide precursor by reaction of the vapor phase with spatially separated graphite, in a closed volume under uniaxial pressure, to form single-crystals of the binary intermetallic clathrates $\text{Na}_8\text{Si}_{46}$ and $\text{Na}_{24}\text{Si}_{136}$. Single-crystal structure refinement for $\text{Na}_8\text{Si}_{46}$ is reported for the first time. For both $\text{Na}_8\text{Si}_{46}$ and $\text{Na}_{24}\text{Si}_{136}$, full occupation of all Si framework sites as well as full Na occupancy in both polyhedra was observed. In addition to comprising a simple method for selective, phase-pure crystal growth of clathrates such as $\text{Na}_8\text{Si}_{46}$ or $\text{Na}_{24}\text{Si}_{136}$ which was previously challenging to achieve, this or similar approaches are applicable in the preparation of new compositions from different alkali-metal precursors.

KEYWORDS: clathrate, intermetallic, crystal growth, silicon, alkali-metal



I. INTRODUCTION

The recent development of novel and unconventional synthetic routes for preparing intermetallic clathrates is motivated by the exceptional structure–property relationships these materials display¹ and potential for solid state energy conversion applications.² Chemical oxidation,³ spark plasma treatment,⁴ high-temperature/high-pressure,⁵ and other approaches⁶ utilizing appropriate crystalline precursors have emerged as effective synthetic tools for preparing new stable and metastable compositions otherwise inaccessible by more conventional solid state synthesis or crystal growth methods. Whereas single crystals are readily grown using established techniques⁷ or flux synthesis⁸ for some representatives, crystal growth of many intermetallic clathrate compositions can be challenging;⁹ in such cases the identification of effective and easily implemented methods for crystal growth is prerequisite to gaining a better understanding of their intriguing structural and physical properties.

The relative chemical simplicity of the prototypical¹⁰ clathrate-I A_8E_{46} and clathrate-II $\text{A}_{24}\text{E}_{136}$ (A = alkali-metal, E = Si or Ge) is ideal for understanding fundamental structure–property relationships in intermetallic clathrates.¹¹ However, synthesis in these binary systems has historically been complicated by the simultaneous formation of two different clathrate structure types (clathrate-I and clathrate-II), which are characterized by nearly identical compositions. Typically

prepared only in microcrystalline form by thermal decomposition of A_4E_4 under vacuum or argon atmosphere,^{10,12–14} achieving a homogeneous product of either phase remains nontrivial.¹⁵ Moreover, a rational, generally applicable, and accessible method for selective, phase pure crystal growth of these materials has not yet been proposed. Very recently, $\text{Na}_{24}\text{Si}_{136}$ single crystals were prepared for the first time by an unconventional approach using spark plasma treatment of Na_4Si_4 .⁴ Herein we demonstrate that selective, phase pure, single-crystal growth of either $\text{Na}_8\text{Si}_{46}$ or $\text{Na}_{24}\text{Si}_{136}$ can be achieved by simply maintaining sufficient alkali-metal partial pressures during slow, controlled deprivation of alkali-metal from the respective tetrelide precursor. The approach appears promising for accessing regions of the equilibrium diagram that can be otherwise difficult to reach in such systems due to the divergent properties of the constituent elements.

II. EXPERIMENTAL SECTION

Na metal (99.95%) and Si lump (99.9999%) were used as purchased from Alfa Aesar. Surface contamination of the Na metal was removed

Received: November 1, 2010

Revised: January 24, 2011

Published: February 10, 2011

with a scalpel in a dry, purified N_2 glovebox. Si was also ground under N_2 to promote reaction. Crystalline Na_4Si_4 was prepared by direct reaction of elemental Na and Si in the Na:Si mass ratio 1.1:1 under N_2 in sealed stainless steel vessels at 650 °C for 36 h. Before use for clathrate crystal growth, NaCl powder (99.99%) and graphite flake (99.9%) were dried by heating in high vacuum at 300 °C. After reaction, the crystals are recovered from the unreacted Na_4Si_4 precursor matrix by controlled dissolution of the remaining Na_4Si_4 in ethanol and distilled water under nitrogen atmosphere. Extreme caution should be used since Na_4Si_4 can react explosively with moisture in air.

Single-crystal X-ray diffraction intensity data for both Na_8Si_4 and $Na_{24}Si_{136}$ were collected at 200(2) K on a three-circle diffractometer system equipped with Bruker Smart Apex II CCD area detector using a graphite monochromator and a MoK α fine-focus sealed tube ($\lambda = 0.71073$ Å). Structure refinement for Na_8Si_4 : $R_1 = 0.0110$ for $I > 2\sigma(I)$ and $wR_2 = 0.0254$ for all data; GOF = 1.000; largest peak 0.215 e $^-/\text{\AA}^3$; largest hole -0.120 e $^-/\text{\AA}^3$; calculated density 2.312 g/cm 3 . Structure refinement for $Na_{24}Si_{136}$: $R_1 = 0.0115$ for $I > 2\sigma(I)$ and $wR_2 = 0.0290$ for all data; GOF = 1.000; largest peak 0.203 e $^-/\text{\AA}^3$; largest hole -0.122 e $^-/\text{\AA}^3$; calculated density 2.280 g/cm 3 . Refinement data and results are tabulated in Tables S1–S6 in the Supporting Information (SI).

Powder X-ray diffraction patterns were collected with a Bruker D8 Focus diffractometer in Bragg–Brentano geometry using Cu K α radiation and a graphite monochromator. NIST Si 640c internal standard was used for determination of lattice parameters. Scanning electron micrographs (SEM) were collected using a JEOL JSM-6390LV, and energy dispersive X-ray spectroscopic (EDS) data were collected using an Oxford INCA X-Sight 7582M. From EDS analysis, stoichiometries of $Na_{7(1)}Si_{46}$ and $Na_{23(1)}Si_{136}$ were calculated for clathrate-I and clathrate-II crystals, respectively, consistent with single-crystal structure refinements.

III. RESULTS AND DISCUSSION

By example of the Na–Si system which has historically received the most attention,⁹ we have taken certain factors into consideration in order to guide our approach: (i) Linked to the relatively high vapor pressure of Na over the compound, thermal decomposition of the precursor Na_4Si_4 under dynamic vacuum or inert atmosphere in open vessels occurs at relatively low temperatures (350–450 °C, depending on vessel and environment), resulting in microcrystalline products.^{12–15} (ii) Na_4Si_4 is stable (with respect to decomposition) under sufficient Na partial pressure in closed (i.e., sealed) vessels and melts congruently at 800 °C.¹⁶ (iii) Since the clathrate products are deficient in Na relative to Na_4Si_4 (which is a line compound), nucleation and growth for both Na_8Si_4 and $Na_{24}Si_{136}$ will likely require a controlled and continuous shift toward the Si-rich composition and mass transport must take place. In light of these considerations, if a relatively high partial pressure of Na could be maintained and adequate mass transport facilitated upon crystal nucleation as the composition of the precursor is continuously changed, growth of single crystals might be achieved.

In our approach, alkali-metal is slowly removed from Na_4Si_4 precursor by reaction of the vapor phase with spatially separated graphite, in an effectively closed volume under uniaxial pressure. A customized reaction vessel comprising a simple punch and die design was constructed such that uniaxial pressure was applied to the specimen while heated in a tube furnace. The Na_4Si_4 precursor is coarsely ground under dry nitrogen atmosphere and loaded into a stainless steel die assembly, along with high purity graphite flake loaded above and below the Na_4Si_4 precursor. (**Caution!** Na_4Si_4 can react explosively with moisture and air. Use appropriate precautions.) To prevent the adhesion between graphite and clathrate crystals, which occurred on first attempts, a 1 mm thick layer of dry NaCl powder is

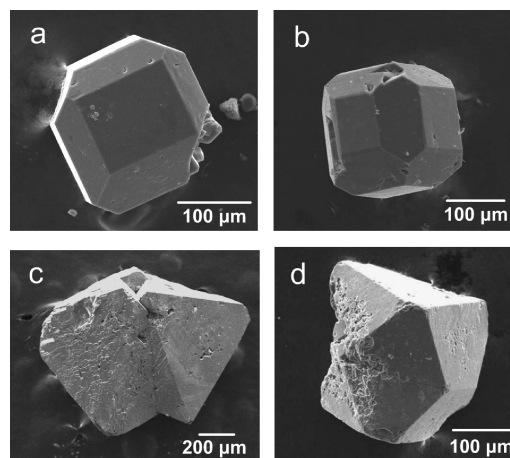


Figure 1. Scanning secondary electron micrographs of Na_8Si_{46} single crystals (a and b) grown at 585 °C and $Na_{24}Si_{136}$ single crystals (c and d) grown at 665 °C. The reaction time for both phases was 8 h.

introduced between the Na_4Si_4 precursor and graphite. The NaCl layer serves as an effective passive physical barrier to direct reaction between graphite and Na_4Si_4 but allows diffusive exchange of Na via the vapor phase. This C–NaCl– Na_4Si_4 –NaCl–C “sandwich” is encapsulated on all sides by graphite foil to impede the escape of Na vapor, then compressed and clamped under uniaxial pressure of 115 MPa at room temperature. The entire assembly is introduced into a fused silica ampule, coupled to a vacuum system, evacuated to 10^{-6} Torr, and heated at the desired reaction temperature under dynamic vacuum.

As shown in Figure 1, by reaction at appropriate temperature, selective single crystal growth of both Na_8Si_{46} and $Na_{24}Si_{136}$ is achieved. The clathrate product of the reaction can be readily separated from the remaining unreacted Na_4Si_4 precursor by careful, controlled dissolution under inert atmosphere in ethanol and then distilled water (**Caution!** Na_4Si_4 can react explosively with moisture and air. Use appropriate precautions.) EDS detected only Na and Si to be present in the crystals. Na_8Si_{46} crystals are repeatedly observed to form as truncated cubes, whereas $Na_{24}Si_{136}$ formed with pyramidal habit. Twinned crystals as shown in Figure 1c are observed for $Na_{24}Si_{136}$, but rarely for Na_8Si_{46} . These observations are consistent with high resolution transmission electron microscopy studies¹⁷ on microcrystalline Na_xSi_{136} ($x < 24$) and Na_8Si_{46} specimens obtained from thermal decomposition of Na_4Si_4 . In spite of the propensity for twinning in this crystal system, relatively large single crystals of $Na_{24}Si_{136}$ are nevertheless obtained.

The effects of temperature and time on the reaction products were studied and it was established that the selectivity in growth of Na_8Si_{46} or $Na_{24}Si_{136}$ is accomplished by merely changing the reaction temperature. For reactions run at 500 °C for 8 h, the formation of either clathrate phase was not observed. Between 580 and 590 °C, clathrate-I Na_8Si_{46} was found to exclusively form, whereas between 660 and 670 °C crystal growth of clathrate-II $Na_{24}Si_{136}$ occurred instead. Elucidated by the powder X-ray diffraction (XRD) patterns shown in Figure 2, phase pure $Na_{24}Si_{136}$ (cubic lattice parameter $a = 14.7167(8)$ Å) and Na_8Si_{46} ($a = 10.1962(9)$ Å) specimens are synthesized by reacting for 8 h at 665 and 585 °C, respectively. The typical yield for relatively large crystals was 8.5% and 6% for Na_8Si_{46} and $Na_{24}Si_{136}$, respectively, relative to the starting mass of the precursor, and can be increased by increasing the reaction time. Simulated powder XRD patterns, based on the respective

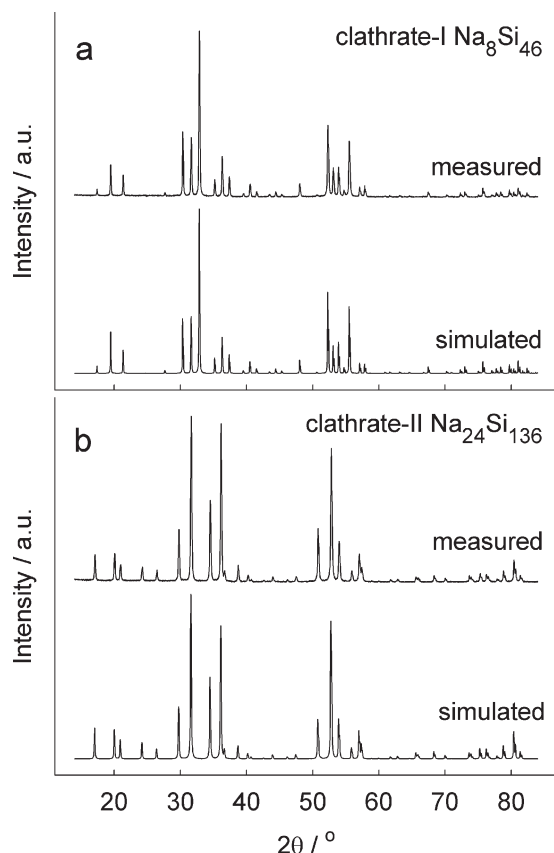


Figure 2. Measured and simulated powder X-ray diffraction patterns for (a) $\text{Na}_8\text{Si}_{46}$ and (b) $\text{Na}_{24}\text{Si}_{136}$ prepared at 585 and 665 °C, respectively, collected from crushed single crystal specimens. No impurity phases are detected.

refined crystal structures obtained from single crystal XRD (vide infra), are also shown for reference.

Preliminary magic angle spinning ^{23}Na nuclear magnetic resonance data (not shown) corroborates the phase purity of the products by the absence of chemical shifts in the spectra originating from the other corresponding clathrate phase. The ease with which high quality, phase pure specimens are obtained illustrates the effectiveness of the method for selective synthesis of the desired clathrate-I or clathrate-II phase, respectively, which has traditionally been highly challenging using the known synthetic routes. Moreover, this identifies the first method for selective crystal growth of Na–Si clathrate-I and clathrate-II, respectively.

The crystal structures of $\text{Na}_8\text{Si}_{46}$ and $\text{Na}_{24}\text{Si}_{136}$ were accurately refined by single crystal X-ray diffraction studies, which further confirmed the identity and phase purity of the single crystals. The resulting refined crystal structures are depicted in Figure 3. In both structures, the silicon framework is characterized by three crystallographically independent Si atoms, which form two different coordination cages for the Na guests: Si_{20} and Si_{24} in $\text{Na}_8\text{Si}_{46}$ and Si_{20} and Si_{28} in $\text{Na}_{24}\text{Si}_{136}$. The single-crystal structure refinement for $\text{Na}_8\text{Si}_{46}$ is reported here for the first time. In both phases, full occupation of all Si framework sites was observed, and both cages in the two clathrate structures were found to be fully occupied by the Na guests confirming stoichiometric compositions. Substantial disorder is observed for the guest Na@Si_{28} in $\text{Na}_{24}\text{Si}_{136}$, in agreement with a rattling phonon

mode and off-centring associated with this guest.^{4,11b,18,19} Similar disorder for Na@Si_{20} in $\text{Na}_{24}\text{Si}_{136}$ and Na@Si_{20} and Na@Si_{24} in $\text{Na}_8\text{Si}_{46}$ was not observed, and can be understood in terms of the relative sizes of the guest and cage (cf. SI).

It is noteworthy that direct synthesis and crystal growth of these phases from the elements is unsuccessful and the available Na–Si equilibrium diagram describes only a eutectic between Na_4Si_4 and Si and the absence of the clathrate phases.¹⁶ In spite of these considerations, the present approach enables the growth of relatively large single crystals of both $\text{Na}_8\text{Si}_{46}$ and $\text{Na}_{24}\text{Si}_{136}$. We propose (cf. Figure 4) that Na vapor, released from the Na_4Si_4 precursor, reacts with the spatially separated graphite, forming intercalation compounds Na_xC . Powder X-ray diffraction of the graphite flake recovered after the reaction confirms the presence of a mixture of stages of Na intercalated graphite (SI Figure S2). Presumably, the vapor pressure of Na over the intercalated graphite is less than that over Na_4Si_4 , such that the intercalation of the graphite results in further release of Na from the precursor in order to locally maintain the Na vapor pressure over the precursor (Le Chatelier's principle). Continued reaction to form Na_xC continuously drives the composition in the precursor Si-rich. Nucleation of the respective clathrate phase ensues as the Na content of the sintered body is reduced, and the continuously applied uniaxial pressure facilitates mass transport between precursor and growing crystal. The rates of these dynamic processes are expected to be limited by mass exchange through the vapor phase, as well as diffusion of Na out of the precursor and the reaction kinetics of Na_xC formation. Precursor approaches such as this may prove useful to access regions of equilibrium diagrams that are otherwise difficult to reach due to the difficulty in controlling composition during nucleation and growth.

The approach can also be employed for the crystal growth of other intermetallic clathrates. We have therefore applied our approach to other alkali-metal tetrelide precursors, using similar conditions to those described above. Selective crystal growth of clathrate-I K_8Si_{46} (Figure 5, $a = 10.272(4)$ Å) and clathrate-II $\text{K}_{24-x}\text{Si}_{136}$ ($a = 14.723(1)$ Å) was also successfully achieved from the precursor K_4Si_4 . Structural and physical properties of these crystals will be reported in detail elsewhere.

To our knowledge, the $\text{K}_{24-x}\text{Si}_{136}$ clathrate is synthesized unequivocally¹⁵ for the first time, reflecting substantial promise of this approach to obtain novel clathrate-II compositions, of which only a handful are presently known.⁹ Single crystals of the ternary clathrate-II $\text{Na}_{16}\text{Cs}_8\text{Ge}_{136}$ ²⁰ of significantly larger size than those typically obtained from direct reaction of a stoichiometric mixture of the elements are also prepared from the ternary precursor NaCsGe_2 . We expect the method to be generally applicable to a variety of precursors; further investigation of the mechanisms behind the growth process and the application to other material systems are currently underway by the authors.

IV. SUMMARY AND CONCLUSIONS

We have described here a straightforward method for the selective single crystal growth of the intermetallic clathrates A_8Si_{46} and $\text{A}_{24}\text{Si}_{136}$ ($\text{A} = \text{Na}, \text{K}$) by controlled alkali deprivation from bulk crystalline A_4Si_4 precursors. While we have not yet pursued such possibilities, we speculate that other techniques (e.g., mechanical control of the alkali partial pressure, as opposed to chemical) should also be effective, assuming that mass transport is achieved in the precursor to allow growth of the target

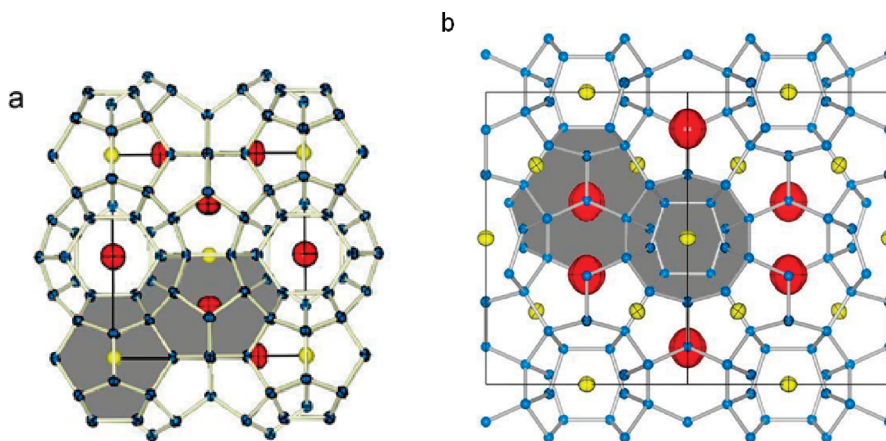


Figure 3. Crystal structures of (a) cubic $\text{Na}_8\text{Si}_{46}$ viewed down $[100]$ and (b) cubic $\text{Na}_{24}\text{Si}_{136}$ viewed down $[110]$, determined from single crystal X-ray diffraction refinements. Silicon atoms are shown in blue, $\text{Na}@Si_{20}$, in yellow, and $\text{Na}@Si_{24}$ (a) and $\text{Na}@Si_{28}$ (b), in red. Na in the Si_{28} cage in $\text{Na}_{24}\text{Si}_{136}$ was refined as off-center at the $48f$ site. Ellipsoids are shown for 99% probability.

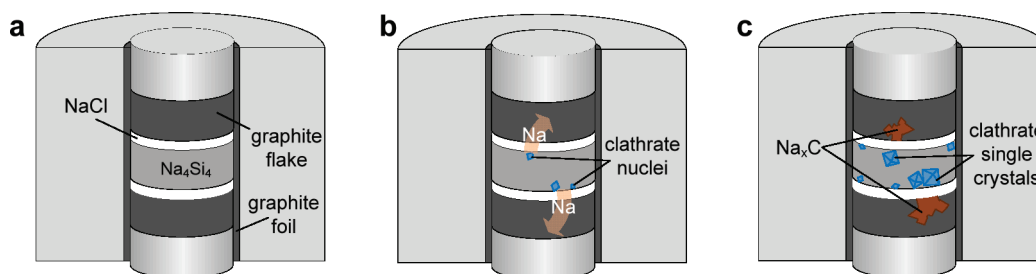


Figure 4. Simple schematic illustrating the presumed $\text{Na}_8\text{Si}_{46}$ and $\text{Na}_{24}\text{Si}_{136}$ crystal growth processes. (a) Initial precursor configuration, under uniaxial pressure in the stainless steel punch and die. (b) Local composition change and nucleation of the clathrate phase. (c) Formation of intercalated graphite and clathrate crystal growth.

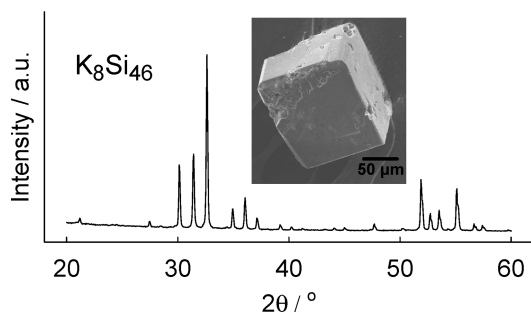


Figure 5. X-ray powder diffraction pattern collected from crushed K_8Si_{46} single crystals. (inset) SEM image of a K_8Si_{46} single crystal.

phase. The application of this or similar approaches to explore the possibilities of preparing intriguing elemental structures that have very recently been obtained²¹ from precursors such as Na_4Si_4 may also be of interest.

■ ASSOCIATED CONTENT

S Supporting Information. CIF files, Tables S1–S6, Figures S1 and S2, and details on the single crystal refinements and results. This material is available free of charge via the Internet at <http://pubs.acs.org>.

■ AUTHOR INFORMATION

Corresponding Author

*E-mail: gnolas@usf.edu.

■ ACKNOWLEDGMENT

S.S., M.B., and G.S.N. acknowledge support from the U.S. Department of Energy under Grant No. DE-FG02-04ER46145 for development of the new crystal growth method, SEM and powder XRD measurements, and data analyses. The authors thank Dr. M. Baitinger and Prof. Dr. Yu. Grin for stimulating discussions and Prof. C. R. Bowers for making available preliminary MAS NMR data on $\text{Na}_8\text{Si}_{46}$ and $\text{Na}_{24}\text{Si}_{136}$.

■ REFERENCES

- (1) (a) Kawaji, H.; Horie, H.; Yamanaka, S.; Ishikawa, M. *Phys. Rev. Lett.* **1995**, *74*, 1427–1429. (b) Cohn, J. L.; Nolas, G. S.; Fessatidis, V.; Metcalf, T. H.; Slack, G. A. *Phys. Rev. Lett.* **1999**, *82*, 779–782. (c) Hermann, R. P.; Keppens, V.; Bonville, P.; Nolas, G. S.; Grandjean, F.; Long, G. J.; Christen, H. M.; Chakoumakos, B. C.; Sales, B. C.; Mandrus, D. *Phys. Rev. Lett.* **2006**, *97*, 017401–1–017401–4.
- (2) (a) Nolas, G. S.; Cohn, J. L.; Slack, G. A.; Schujman, S. B. *Appl. Phys. Lett.* **1998**, *73*, 178–180. (b) Shi, X.; Yang, J.; Bai, S.; Yang, J.; Wang, H.; Chi, M.; Salvador, J. R.; Zhang, W.; Chen, L.; Wong-Ng, W. *Adv. Func. Mater.* **2010**, *20*, 755–763.
- (3) (a) Guloy, A. M.; Ramlau, R.; Tang, Z.; Schnelle, W.; Baitinger, M.; Grin, Yu. *Nature* **2006**, *443*, 320–323. (b) Böhme, B.; Guloy, A.

Tang, Z.; Schnelle, W.; Burkhardt, U.; Baitinger, M.; Grin, Yu. *J. Am. Chem. Soc.* **2007**, *129*, 5348–5349. (c) Neiner, D.; Okamoto, N. L.; Condrón, C. L.; Ramasse, Q. M.; Yu, P.; Browning, N. D.; Kauzlarich, S. M. *J. Am. Chem. Soc.* **2007**, *129*, 13857–13862.

(4) Beekman, M.; Baitinger, M.; Borrmann, H.; Schnelle, W.; Meier, K.; Nolas, G. S.; Grin, Yu. *J. Am. Chem. Soc.* **2009**, *131*, 9642–9643.

(5) (a) San-Miguel, A.; Toulemonde, P. *High Press. Res.* **2005**, *25*, 159–185. (b) Wosylus, A.; Veremchuk, I.; Schnelle, W.; Baitinger, M.; Schwarz, U.; Grin, Yu. *Chem.—Eur. J.* **2009**, *15*, 5901–5903.

(6) Kalzoglou, A.; Ponou, S.; Fässler, T. F. *Eur. J. Inorg. Chem.* **2008**, 4507–4510.

(7) (a) Sales, B. C.; Chakoumakos, B. C.; Jin, R.; Thompson, J. R.; Mandrus, D. *Phys. Rev. B* **2001**, *63*, 245113–1–245113–8. (b) Christensen, M.; Abrahamsen, A. B.; Christensen, N. B.; Juranyi, F.; Andersen, N. H.; Lefmann, K.; Andreasson, J.; Bahl, C. R. H.; Iversen, B. B. *Nat. Mater.* **2008**, *7*, 811–815.

(8) (a) Condrón, C. L.; Martin, J.; Nolas, G. S.; Piccoli, P. M. B.; Schultz, A. J.; Kauzlarich, S. M. *Inorg. Chem.* **2006**, *45*, 9381–9386. (b) Tanaka, T.; Onimaru, T.; Suekuni, K.; Mano, S.; Fukuoka, K.; Yamanaka, S.; Takabatake, T. *Phys. Rev. B* **2010**, *81*, 165110–1–165110–6.

(9) Beekman, M.; Nolas, G. S. *J. Mater. Chem.* **2008**, *18*, 842–851.

(10) Kasper, J. S.; Hagenmüller, P.; Pouchard, M.; Cros, C. *Science* **1965**, *150*, 1713.

(11) (a) Tse, J. S.; Uehara, K.; Rousseau, R.; Ker, A.; Ratcliffe, C. I.; White, M. A.; MacKay, G. *Phys. Rev. Lett.* **2000**, *85*, 114–117. (b) Beekman, M.; Schnelle, W.; Borrmann, H.; Baitinger, M.; Grin, Yu.; Nolas, G. S. *Phys. Rev. Lett.* **2010**, *104*, 018301–1–018301–4.

(12) Cros, C.; Pouchard, M.; Hagenmüller, P. *J. Solid State Chem.* **1970**, *2*, 570.

(13) (a) Reny, E.; Gravereau, P.; Cros, C.; Pouchard, M. *J. Mater. Chem.* **1998**, *8*, 2839. (b) Ramachandran, G. K.; Dong, J. J.; Diefenbacher, J.; Gryko, J.; Marzke, R. F.; Sankey, O. F.; McMillan, P. F. *J. Solid State Chem.* **1999**, *145*, 716. (c) Horie, H.; Kikudome, T.; Teramura, K.; Yamanaka, S. *J. Solid State Chem.* **2009**, *182*, 129. (d) Beekman, M.; Nenghabi, E. N.; Biswas, K.; Myles, C. W.; Baitinger, M.; Grin, Yu.; Nolas, G. S. *Inorg. Chem.* **2010**, *49*, 5338–5340.

(14) Schäfer, R.; Klemm, W. Z. *Anorg. Allg. Chem.* **1961**, *312*, 214.

(15) von Schnering, H. G.; Somer, M.; Kaupp, M.; Carrillo-Cabrera, W.; Baitinger, M.; Schmeding, A.; Grin, Yu. *Angew. Chem.* **1998**, *37*, 2359.

(16) Morito, H.; Yamada, T.; Ikeda, T.; Yamane, H. *J. Alloys Comp.* **2009**, *480*, 723–726.

(17) Nistor, L.; van Tendeloo, G.; Amelinckx, S.; Cros, C. *Phys. Status Solidi A* **1994**, *146*, 119.

(18) Brunet, F.; Mélinon, P.; San-Miguel, A.; Kéghélian, P.; Perez, A.; Flank, A. M.; Reny, E.; Cros, C.; Pouchard, M. *Phys. Rev. B* **2000**, *61*, 16550.

(19) Beekman, M.; Hermann, R. P.; Möchel, A.; Juranyi, F.; Nolas, G. S. *J. Phys.: Condens. Matter* **2010**, *22*, 355401.

(20) (a) Bobev, S.; Sevov, S. C. *J. Am. Chem. Soc.* **1999**, *121*, 3795–3796. (b) Bobev, S.; Sevov, S. C. *J. Solid State Chem.* **2000**, *92*, 153–155. (c) Nolas, G. S.; Vanderveer, D. G.; Wilkinson, A. P.; Cohn, J. L. *J. Appl. Phys.* **2002**, *91*, 8970–8973.

(21) Morito, H.; Yamane, H. *Angew. Chem., Int. Ed.* **2010**, *49*, 3638–3641.